

# **Warm Dense Matter Theory\***

**2008 Warm Dense Matter Winter School  
Lawrence Berkeley National Laboratory  
The University of California  
Berkeley, California  
January 11, 2008**



**Stephen B. Libby  
Theory & Modeling Group Leader  
V Division  
Physical Sciences Directorate  
Lawrence Livermore National Laboratory**



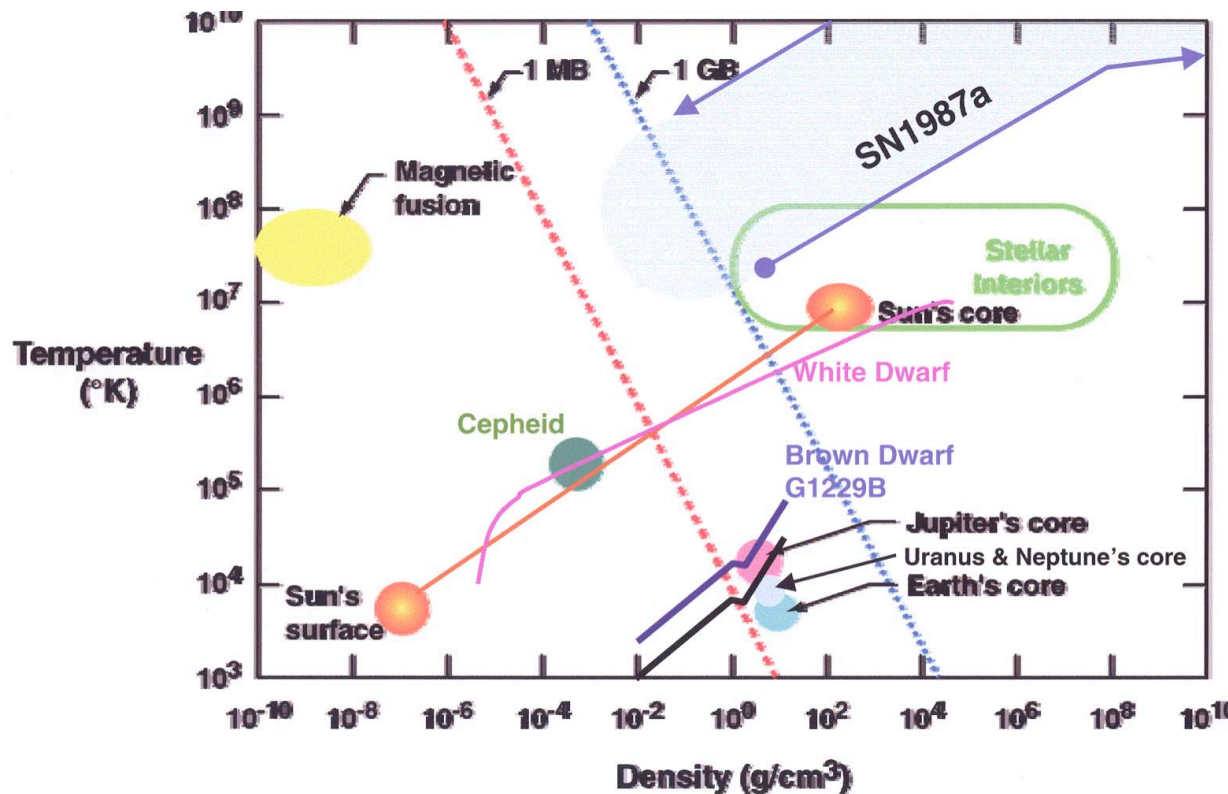
\* LLNL-PRES-400542. This work was performed under the auspices of the U.S. Department of Energy by  
Lawrence Livermore National Laboratory under Contract DE-AC52-07NA27344.

# Warm Dense Matter Theory - Outline



- A little philosophy: in **applications** - **plasma ‘heat engines’** - we seek to control energy transfer. In **basic science** - e.g. astrophysics, possible strange ‘continuations’ of condensed matter phenomena - we seek to understand it.
- Dimensionless parameters (degeneracy, plasma coupling, transport, configuration complexity, etc.) characterize Warm Dense Matter as the boundary between Condensed Matter and High Energy Density Plasma Physics. **In Condensed Matter the really interesting phenomena & theoretical challenges deal with how atoms interact subtly in space. In HED physics, it is often a good approximation to assume individual ions only know about the surrounding plasma sea. But heat turns on lots of ion configurations!**
- ‘INFERNO’ & PURGATORIO single ion in jellium - Detailed EOS and transport models for High Energy Density / WDM Physics - Applications. Limitations.
- PARADISO: multi-center ions in plasma supercell → WDM/condensed matter
- Other approaches - ACTEX, Thermal Field Theory

# High Energy Density Physics is the Study and Application of Matter and Energy with Pressure $> 1$ Megabar $\sim 1$ eV/particle at Solid Density. WDM is condensed boundary.



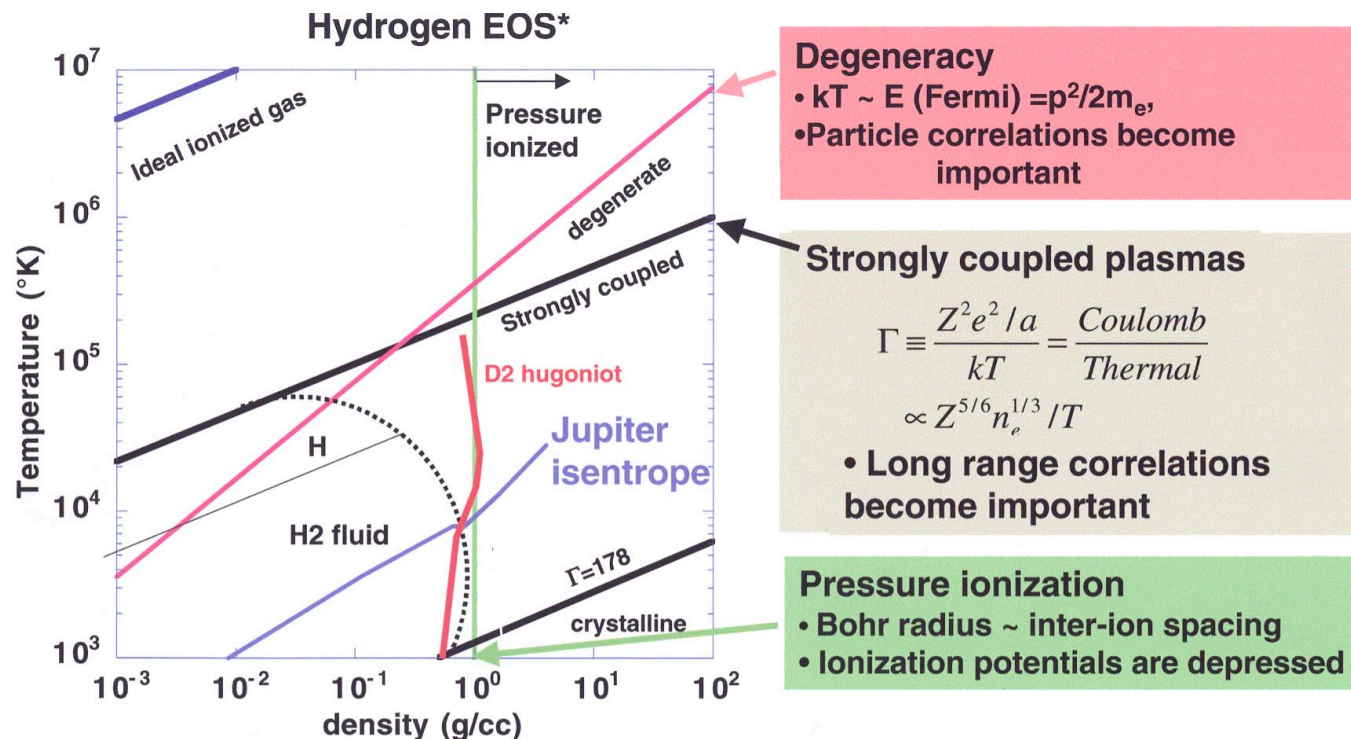
- $P \geq 1$  Mb phenomena: strong ionization, collisionality, importance of radiative energy transfer.

- unless stabilized by gravity - fast transient hydrodynamic instabilities - shocks, interface instabilities

- $P_{\text{air}} = 10^6 \text{ ergs/cc} = 1 \text{ bar} = 10^5 \text{ Pascal (Pa)}$

• Inertial fusion ignition hot spot:  $\rho = 60 \text{ gm/cc}$   $P = 2 (1.4 \cdot 10^{31} / \text{m}^3) \cdot 10 \text{ keV} \cdot (1.6 \cdot 10^{-19} \text{ J/eV}) = 4.5 \cdot 10^{16} \text{ Pa} \approx (1/2) \text{ Terabar ! (Not Warm Dense Matter!)}$

# The Hydrogen Equation of State Illuminates some (but not all!) of the Regimes of High Energy Density Physics and its Warm Dense Matter 'Edge.'



- Isentrope of Jupiter is strongly coupled and degenerate, and crosses the molecular and pressure ionized regimes

\*Saumon et al. 1995 ApJS. 99. 713

- Degeneracy parameter is  $h^2/2m_e \beta n_e^{2/3}$
- $\Gamma \sim (n_e \lambda_D^3)^{-2/3}$
- Generally speaking, as  $T$  goes up, subtle spatial correlations and exchange become less important.
- But, for  $Z \gg 1$  lots of excited states!



# Is 'Warm Dense Matter' a Distinct Phase or Merely an Adiabatic Interpolation Between Condensed Matter and Plasma Physics? Unknown!



- Quantum correlation, competing states & phases distinguished by thermal or quantum singularities prevent adiabatic continuation in condensed matter (superfluids, magnetic phases, spin glass, localization, quantum-Hall, etc.) - usually the province of low temperature physics.
- Warm Dense Matter may have very interesting transport regimes (transport singularities can occur even without thermal phase transitions). Also, note interesting ideas about minimum shear viscosity/entropy density  $\sim h/8\pi^2 k_B \sim 6.08 \cdot 10^{-13}$  K-sec. (Kovtun et. al. - PRL 94, 111601, 2005).
- Electron thermal versus radiation transport.
- Growth of configuration complexity as T increases.

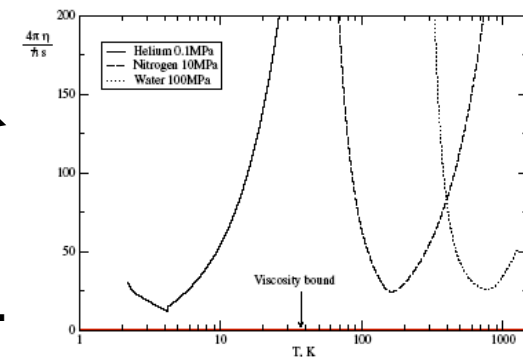


FIG. 2 (color online). The viscosity-entropy ratio for some common substances: helium, nitrogen and water. The ratio is always substantially larger than its value in theories with gravity duals, represented by the horizontal line marked "viscosity bound."

## Warm Dense Matter - Additional Characteristics (2)



- For  $T > 20$  eV &  $\rho \sim 1$  gm/cc radiative flux dominates (Rosseland mfp relevant transport quantity - Marshak waves) - true HED regime.
- $T^4$  term in energy density not relevant here.

$$\frac{d}{dt}(\rho \epsilon_{th} + aT^4) = \frac{d}{dx} \left( \frac{c\lambda_R}{3} \frac{d}{dx} (aT^4) \right) + \frac{V_e \lambda_e}{3} \frac{d}{dx} (\rho \epsilon_{th})$$

- Warm Dense Matter - electron thermal conduction begins to rival radiation.
- Configuration Complexity is another distinction between warm dense matter and HED matter.

- Consider variation of  $\exp(-E(Q^2 \text{ Ryd})/kT)$ . Energy shift adding/subtracting  $q$  electrons is:

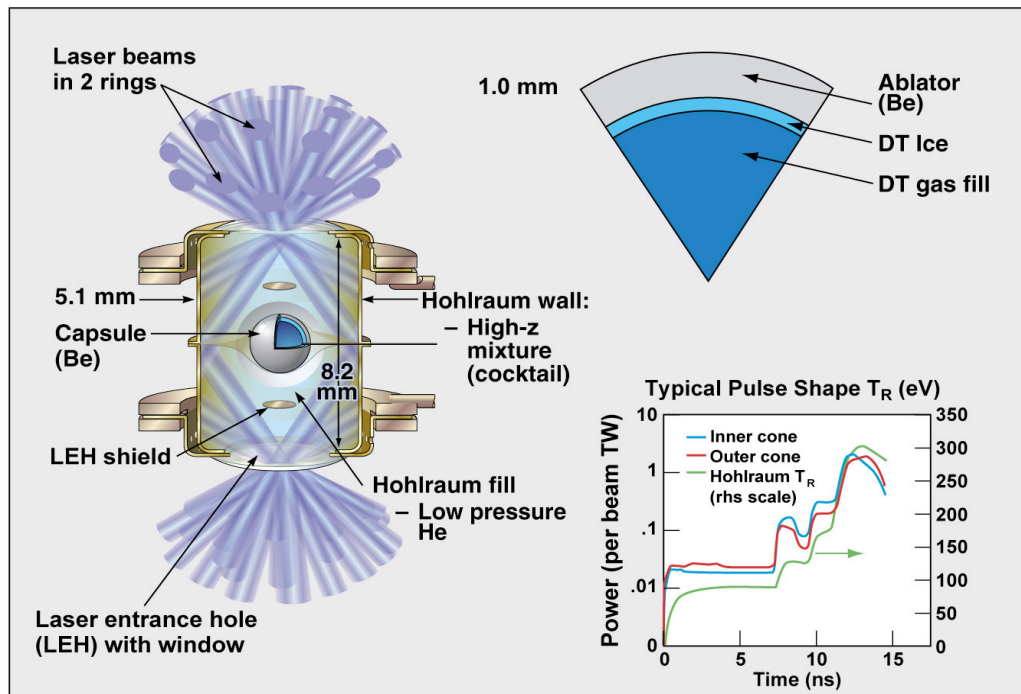
$$\delta E(Q, q) = \left| \frac{E(Q \pm q) - E(Q)}{E(Q)} \right| \approx \left| \frac{(Q \pm q)^2 - Q^2}{Q^2} \right| = \frac{2q}{Q} \left| 1 \pm \frac{q}{2Q} \right| \quad Q = Z_{nuclear} - N_{bound} + 1.$$

- Combinatorial explosion for isoelectronic sequence as  $Z$  increases.

# Inertially Confined Fusion is a Primary Example of a High Energy Density 'Plasma Engine.' What rules control its efficiency? How do the 'degrees of freedom' play? WDM relevant to 'path' to assembly.



## NIF Indirect Drive target point design



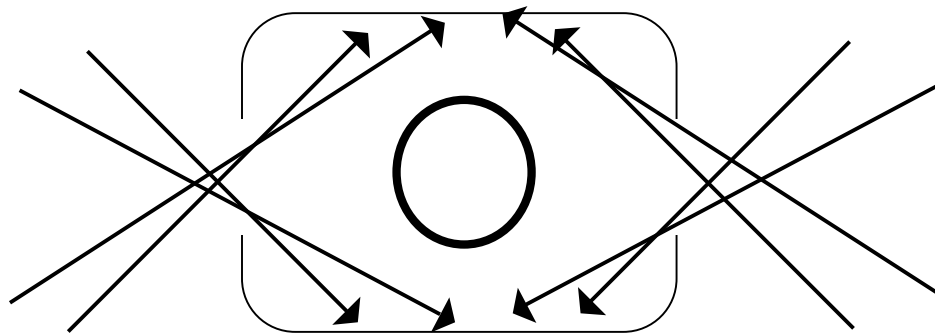
NIF-0505-10823r2  
4/28/10

- For ignition, need HED hot-spot with  $T_{\text{ion}} \sim 10$  keV,  $r R_{\text{HS}} \sim 0.3 \text{ g/cm}^2$   $r_{\text{HS}} \sim 80 \text{ gm/cc}$ .

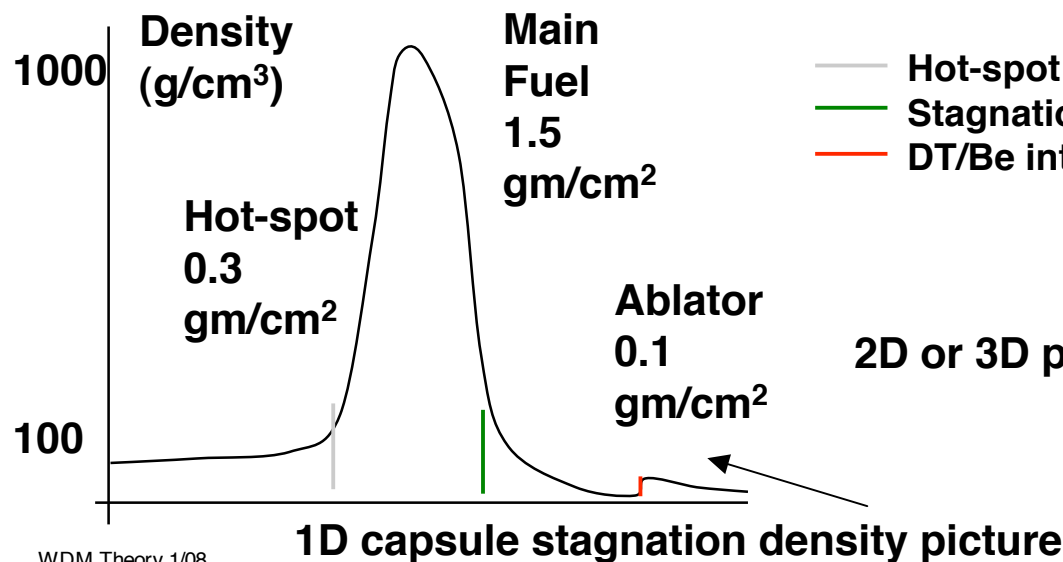
- For confinement need  $r R_{\text{tot}} > 1 \text{ g/cm}^2$  — otherwise hot-spot disassembles before igniting. (burn fraction) =  $r R / [r R + 6]$  assumes burning sphere, don't get there if  $r R_{\text{tot}} < 1 \text{ g/cm}^2$  )

- Ignition begins at  $\sim$ isobaric stagnation.  $R_{\text{DT-Be}} \sim 30$  microns

# Indirect Drive Applies Accurately Timed Laser Heating Pulses to Hohlraum to Make Controlled Quasi-Planckian Soft X-Ray Drive - What Laws Apply to this 'Engine?'

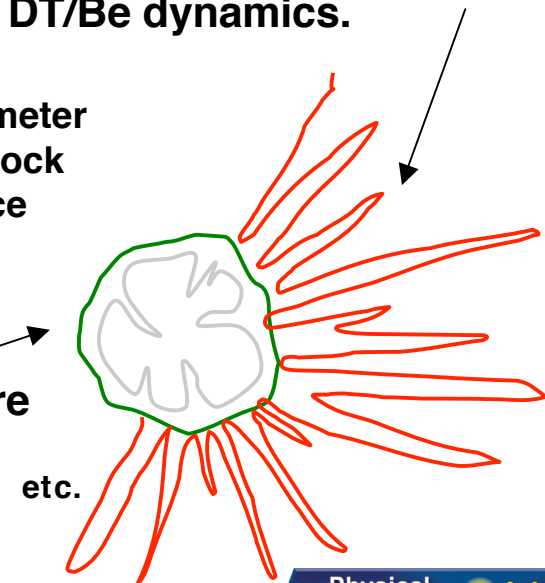


- Goal is keep main DT fuel near adiabat, heating only 2% of DT to center 'hot spot' 10 keV → need only  $\sim 1.25 \times 10^5$  J coupled of  $2 \times 10^6$  J drive. *Is this the most efficient way?*
- Control of hohlraum coupling, shock timing, hydrodynamic instabilities could benefit from comprehensive 'thermal analysis.' WDM relevant to DT/Be dynamics.



- Hot-spot perimeter
- Stagnation shock
- DT/Be interface

2D or 3D picture



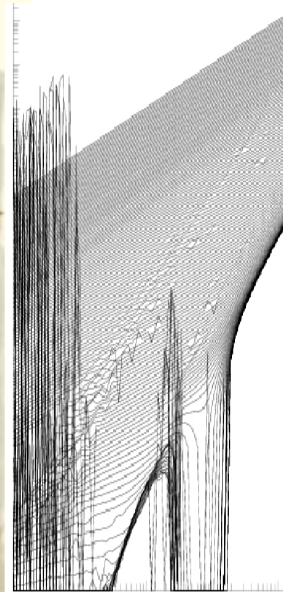


# The Purgatorio code<sup>+</sup> is an Improved Implementation of the Inferno\* Model



## *Inferno*

! Abandon all hope, ye who enter here  
Quasi R-matrix continuum / no tracking  
switches to TFD at high T, crashes at low T

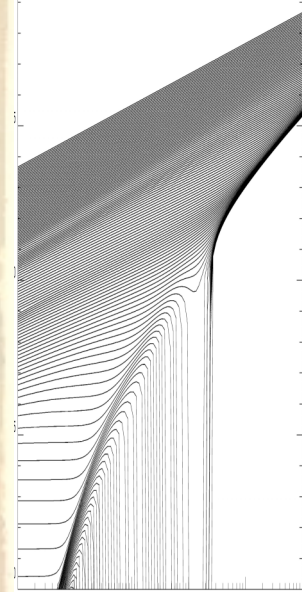


Inferno  $P$  v  $\rho$

\*D. A. Liberman, Phys. Rev. B **20**, 4981 (1979)

## *Purgatorio*

strict convergence criteria (stable at low T)  
accurate continuum wave functions  
careful tracking of continuum resonances via  $\delta(E)$



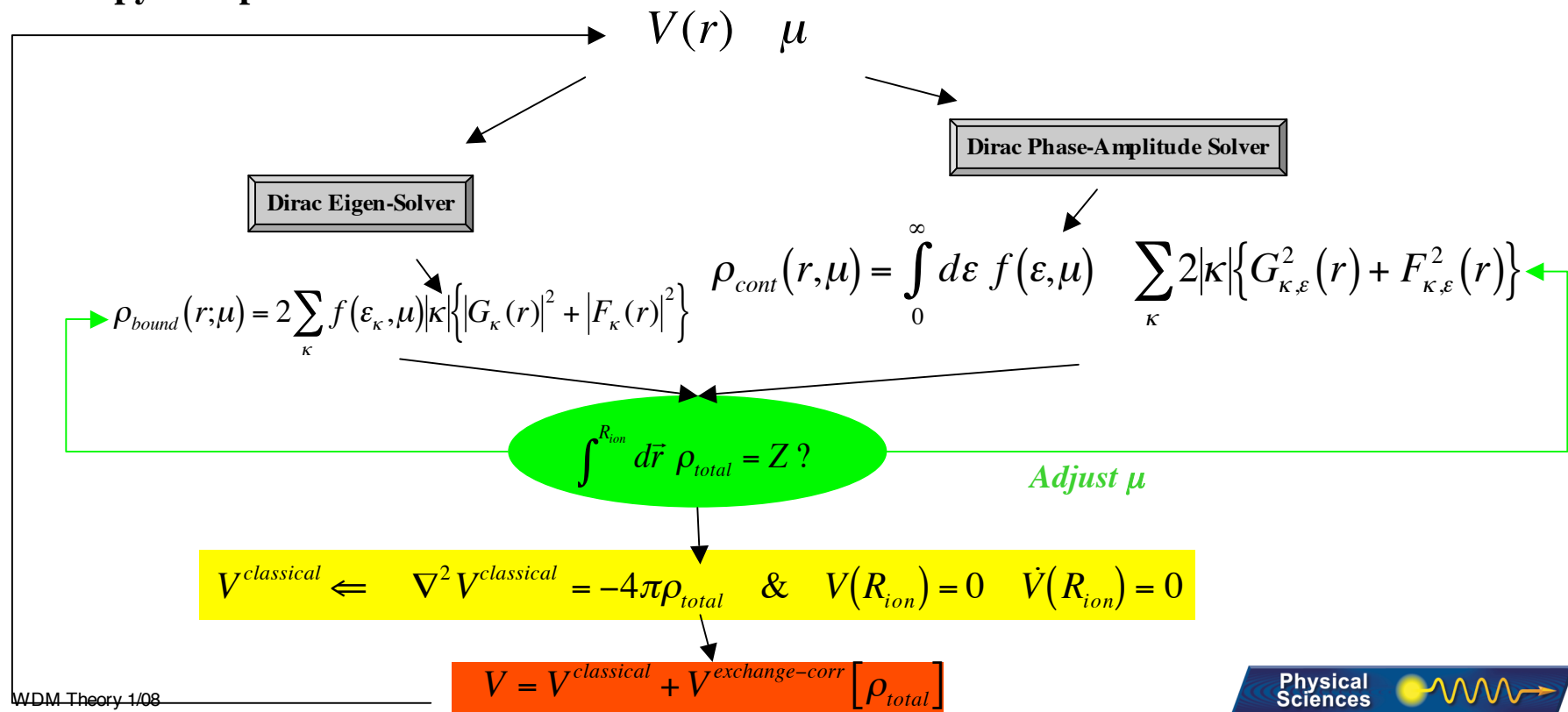
Purgatorio  $P$  v  $\rho$

<sup>+</sup>B. Wilson, V. Sonnad, P. Sterne, and W. Isaacs, JQSRT **99**, 658 (2006).

# The INFERNO & PURGATORIO Kohn-Sham LDA Self-Consistent-Field Algorithm Seeks a Free Energy E-TS Minimum Applying the Single Particle Dirac Equation



- A critical aspect is the accurate calculation of  $\rho(r)$  arising from the continuum
- Solution subject to the constraint of ion-sphere neutrality
- PURGATORIO applies the phase-amplitude method to treat the continuum
- PURGATORIO resonance capturing via greatly improved automated quadrature method
- Entropy is important

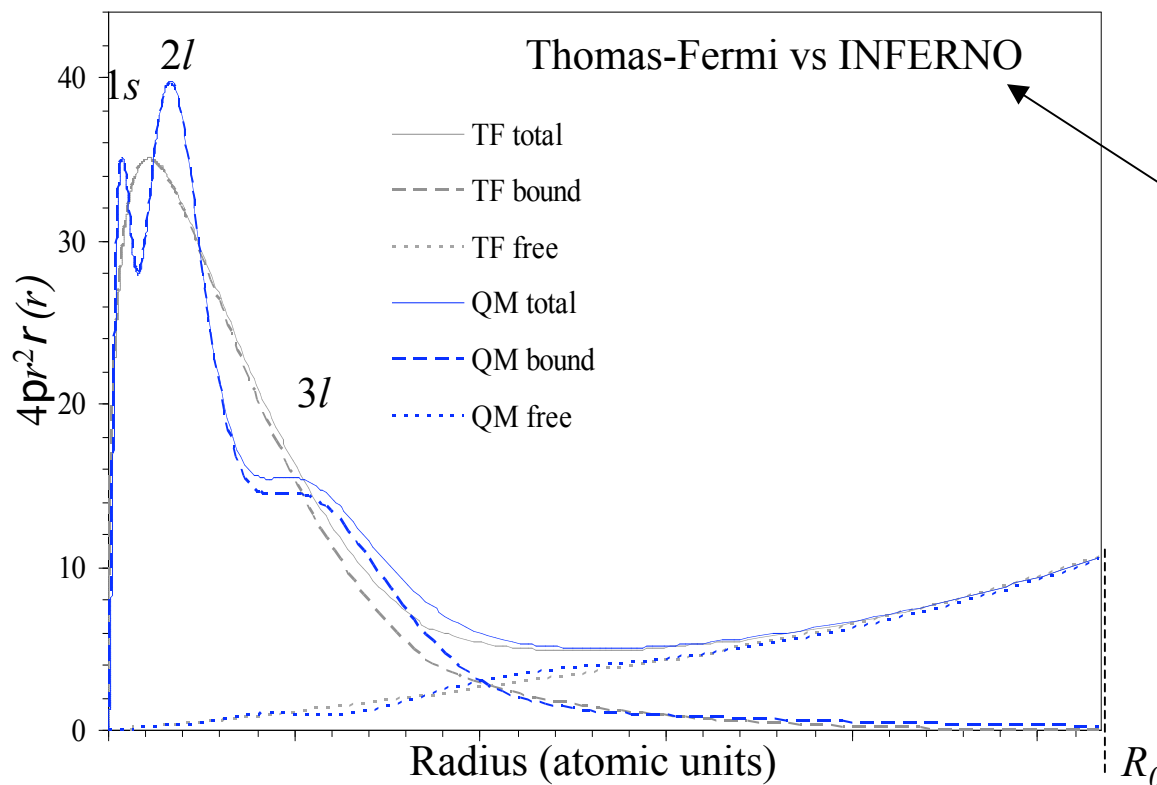


# INFERNO/PURGATORIO Results for Ionic Charge Densities Compared with Thomas Fermi



Thomas-Fermi models have known deficiencies:

- no detailed shell structure
- incorrect treatment of pressure ionization
- the distortion of continuum charge about ion centers is approximate



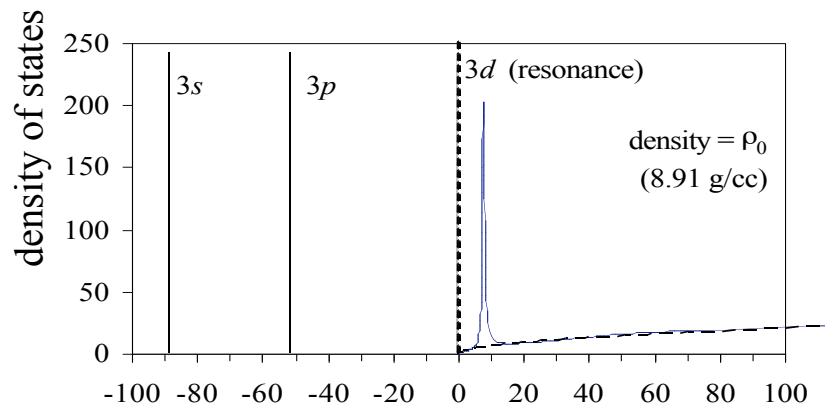
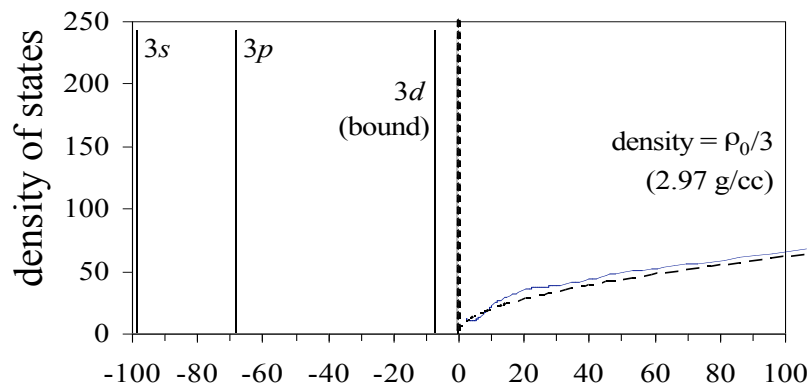
$$4\pi r^2 \rho_{bound}(r) = \sum_{nlj} f(\epsilon_{nlj}, \mu) 2|\kappa| \{P_{nlj}^2(r) + Q_{nlj}^2(r)\}$$

$$4\pi r^2 \rho_{continuum}(r) = \int_0^\infty d\epsilon f(\epsilon, \mu) \sum_{\kappa} 2|\kappa| \{P_{\kappa, \epsilon}^2(r) + Q_{\kappa, \epsilon}^2(r)\}$$

# Resolving continuum resonance structure is critical to the success of the PURGATORIO Improvements to the Inferno Algorithm



Pressure ionization moves bound states into the continuum, forming resonances which introduce large deviations from the ideal density of states:



$$X(\varepsilon)^{ideal} \approx \frac{\Omega}{\pi^2} \sqrt{2\varepsilon}$$

$$X(\varepsilon) = \sum_{\kappa} 2|\kappa| \int_0^{R_0} dr \{p_{\kappa,\varepsilon}^2(r) + Q_{\kappa,\varepsilon}^2(r)\}$$

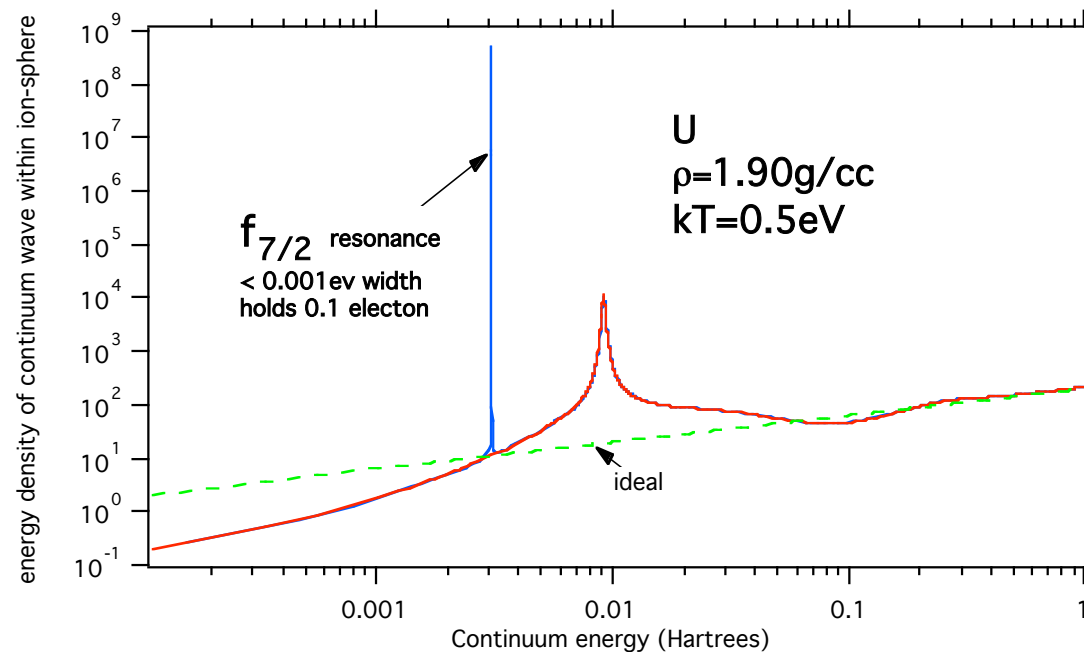
$$= X(\varepsilon)^{ideal} + \frac{2}{\pi} \sum_{\kappa} |2\kappa| \frac{d\delta(\varepsilon)}{d\varepsilon}$$

**Resonances can be extremely narrow but still hold appreciable charge.**

**Finding a converged solution depends on systematic capture of the resonances.**  
 This was by no means guaranteed in the original Inferno code.



## Example Illustrating the Importance of Resonance Capture

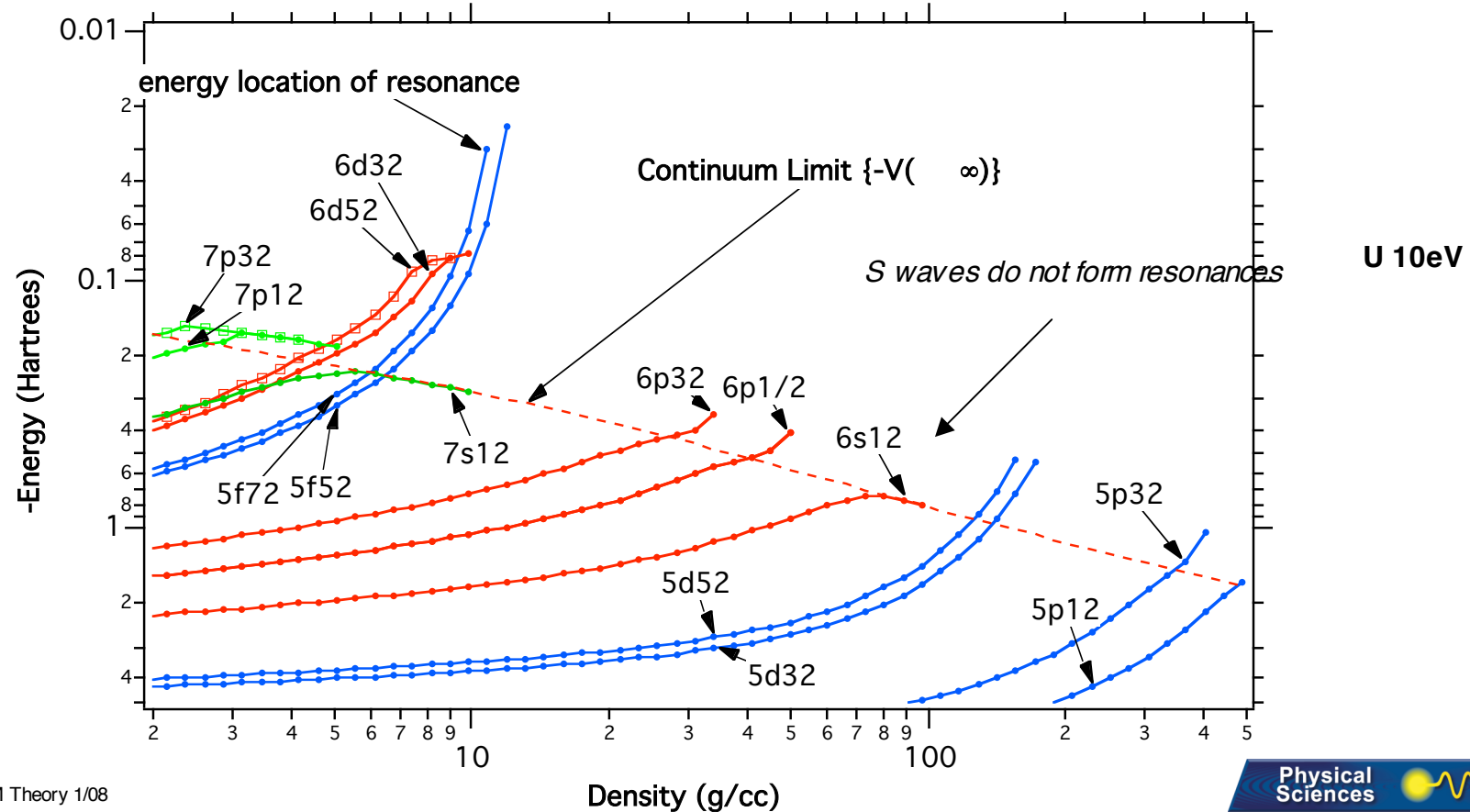


- Code must capture “normalization resonances,” which have nearly entire bound-state-like behavior with exponentially decaying tails that must be matched onto unit amplitude ideal continuum wave at  $R_0$ .
- Resonances are problematic if not they are not systematically caught, since they affect scattering cross sections and can also kick the chemical potential into unending SCF loops.

# Quantum mechanical treatment of pressure ionization in PURGATORIO. In the WDM regime with Weak Ionization, There are also hints of the need to go Beyond PURGATORIO



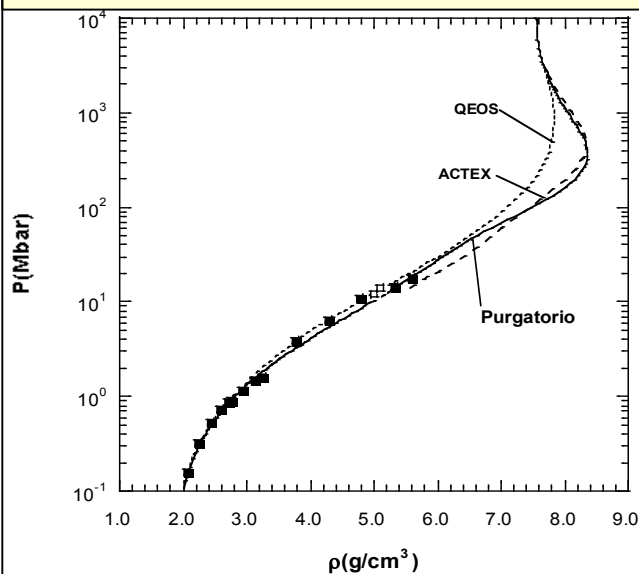
Purgatorio follows bound states as they are pressure ionized and reappear as resonances in the continuum.



# Comparison of Purgatorio EOS results with QEOS and ACTEX - Note interesting case of $\text{Al}_2\text{O}_3$

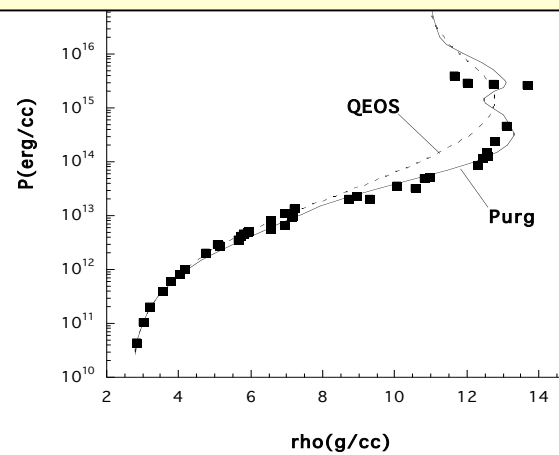


## Beryllium Principal Hugoniot



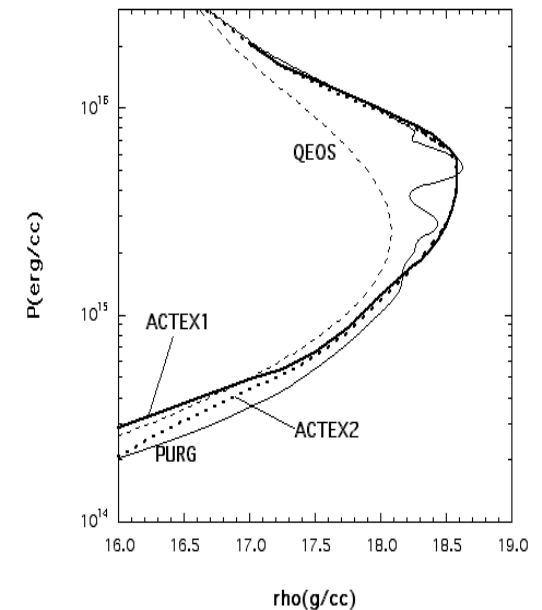
Excellent agreement between  
ACTEX and Inferno-based  
calculations at high pressure

## Aluminum Principal Hugoniot



Atomic shell structure gives  
higher compression and  
structure that a TF model  
cannot represent

## $\text{Al}_2\text{O}_3$ Hugoniot



# The Application Ziman's Resistivity Formula uses PURGATORIO Electronic Information and Added Ionic information.\* Kubo $\sigma(\omega)$ can also be computed.†



$$\eta = -\frac{\Omega}{3\pi} \frac{1}{Z_0 Z_i} \int_0^\infty \frac{\partial f(\varepsilon; \mu, T)}{\partial \varepsilon} \left\{ \int_0^{2p} q^3 \left( \frac{d\sigma(p, \theta)}{d\theta} \right) S(q) dq \right\} d\varepsilon$$

**Electronic components:**

$Z_0$  ( $Z_i$ ) is the number of free (conduction) electrons per ion

$f(\varepsilon)$  is the Fermi function, dependent on the chemical potential  $\mu$

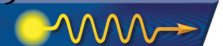
$\frac{d\sigma(p, \theta)}{d\theta}$  is the differential scattering cross section

**Ionic component:**

$S(q)$  is the static ion-ion structure factor

→ *Debye-Hückel, Rinker, MHNC, Percus-Yevick...*

$$\frac{d\sigma(p, \theta)}{d\theta} = \frac{1}{p^2} \left\{ \left| \sum_{\mathbf{k}} |\mathbf{k}| e^{i\delta_{\mathbf{k}}(p)} \sin[\delta_{\mathbf{k}}(p)] P_l(\cos \theta) \right|^2 + \left| \sum_{\mathbf{k}} \frac{|\mathbf{k}|}{i\mathbf{k}} e^{i\delta_{\mathbf{k}}(p)} \sin[\delta_{\mathbf{k}}(p)] P_l^1(\cos \theta) \right|^2 \right\}$$





# Purgatorio Electrical Conductivities are Fairly Consistent with Desjarlais's 'Modified Lee-More' - Low Temperature ( $T < .5$ eV) Values Correspond to $k_f l \ll 1$



- Purgatorio analysis of Cu at  $\sim .1$  gr/cc and  $T \sim .5$  eV, is non-degenerate.
- Ziman conductivity integral has  $k_f \sim 2 \cdot 10^6 \text{ cm}^{-1}$ .
- Ioffe-Regel criterion  $k_f l_{\text{mfp}} < 1$  for metal-insulator transition appears to come into play.

M. P. DESJARLAIS

Contrib. Plasma Phys. 41 (2001) 2-3, 267–270

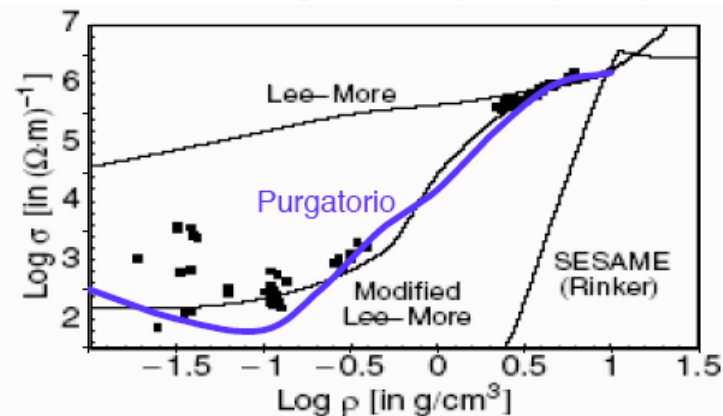
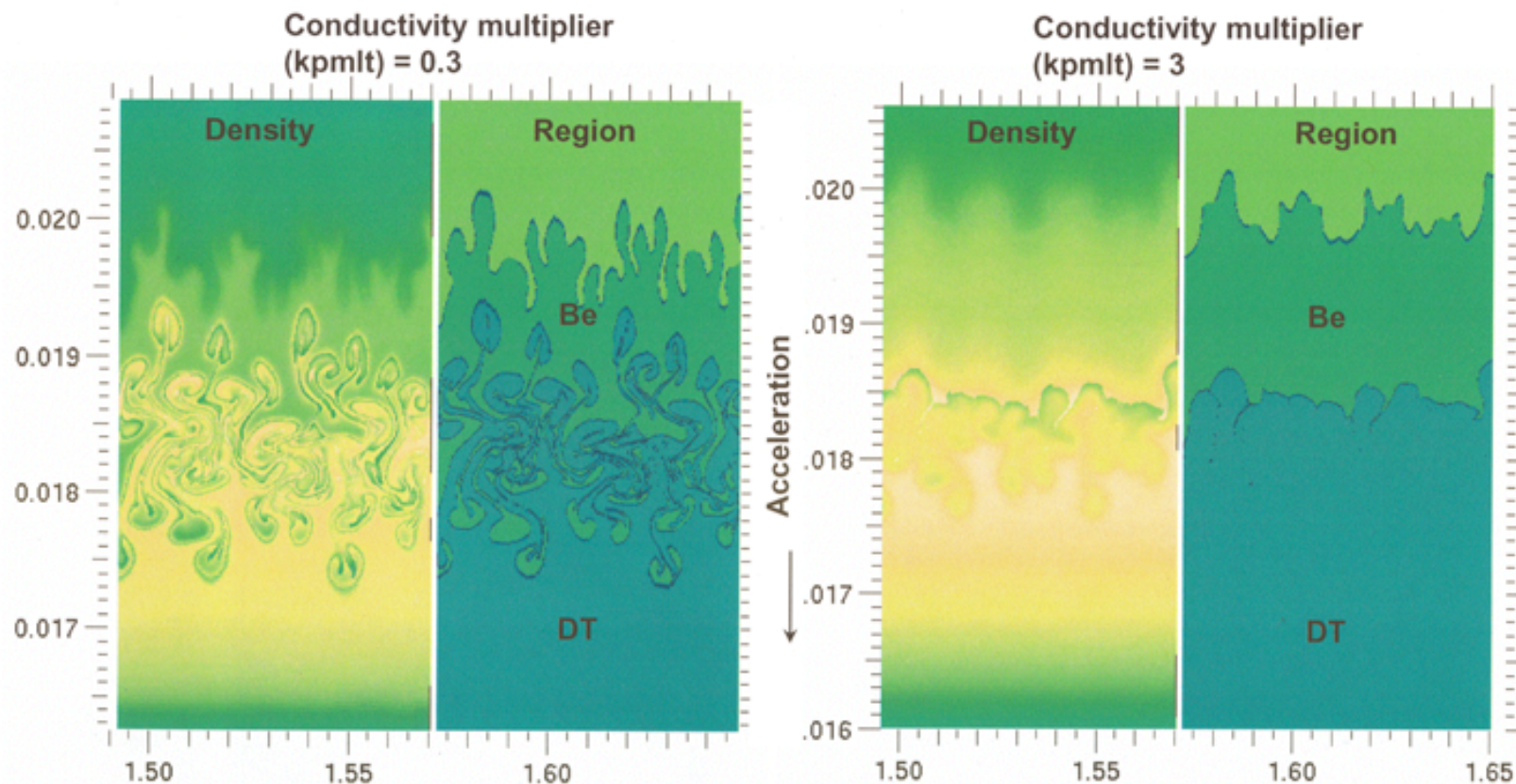


Fig. 1: A comparison between the experimental results of De Silva *et al.* [3], the Lee-More and SESAME (Rinker) conductivities, and the result of our modifications to Lee-More, all for copper at 6000 K.

# Warm Dense Matter Thermal Conductivities of DT and Be Affect the Density Profile and Instability Evolution near the DT:Be Interface in NIF Target Simulations



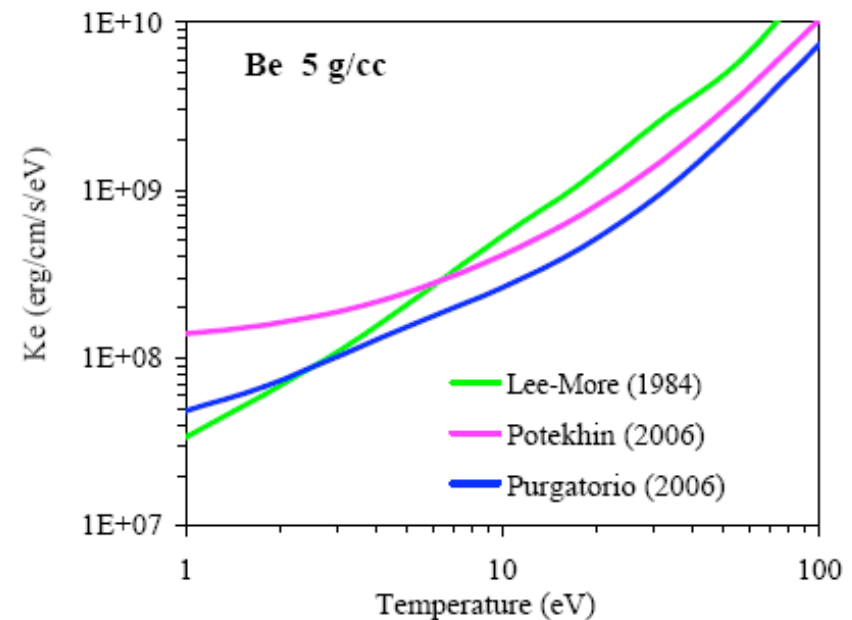
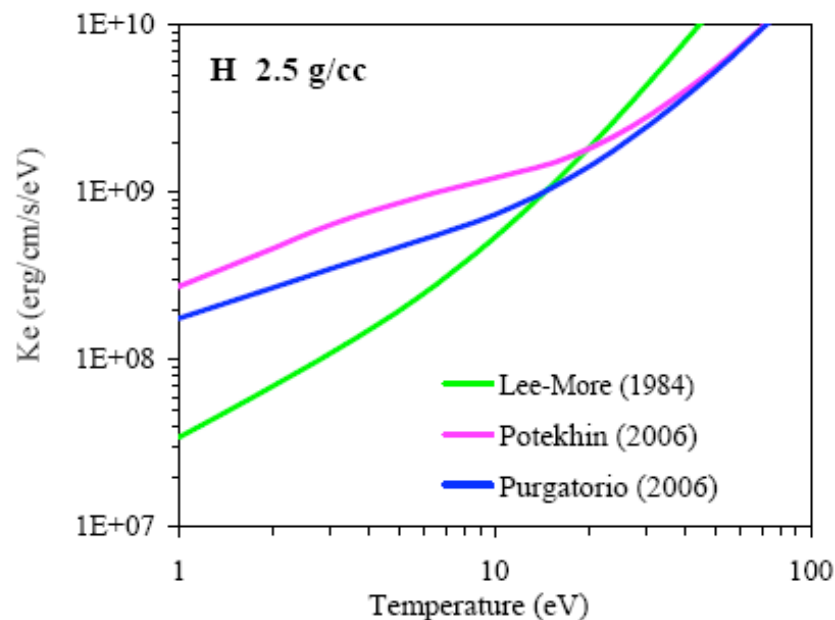
- This sensitivity to uncertainty in thermal conductivity motivated a comparison with the Purgatorio conductivity model.
- Unlike shock timing - *conduction uncertainties cannot be controlled phenomenologically.*

WDM Theory 1/08

Simulations: B. Hammel

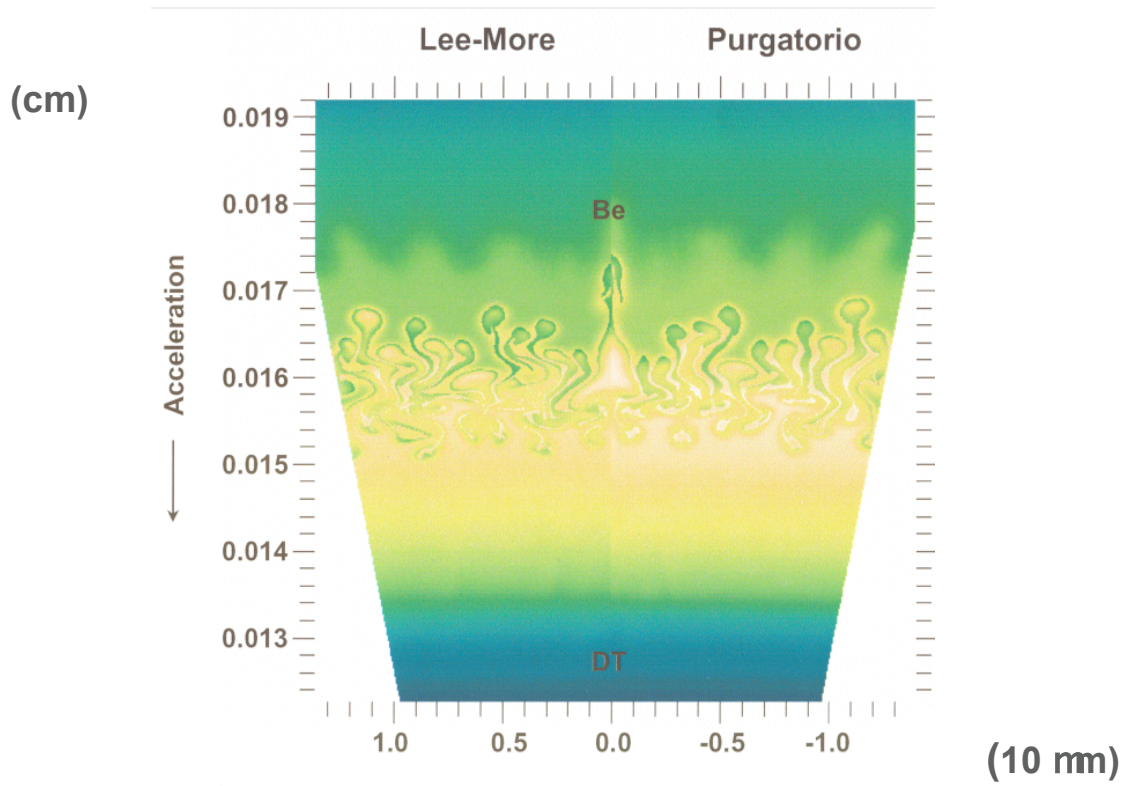


## Purgatorio-based Electron-Thermal Conductivities Differ Significantly from Lee-More values in WDM regime.



- Large Purgatorio Disagreement with Lee-More is due both to cross sections and effective ionization balance (as with electrical conductivity).
- Temperatures of interest for NIF DT:Be interface simulations are  $\sim 3$ - $10$  eV at  $\sim 2$ - $5$  gr/cc

# Comparison of DT:Be Interface Mixing: Applying Purgatorio and Lee-More Values Thermal Conductivities.



Simulations: B. Hammel

DT:Be interface near peak  
implosion velocity (14.8 ns)

- Preliminary analysis of the effects of H and Be conductivity increase/decrease compensate in this case - but cannot guarantee by experimental tuning.



# The Path from a Single Average Ion Immersed in Electron Jellium to a Multi-Center Ensemble of Ions Brings us to 'PARADISO.'



*Purgatorio*

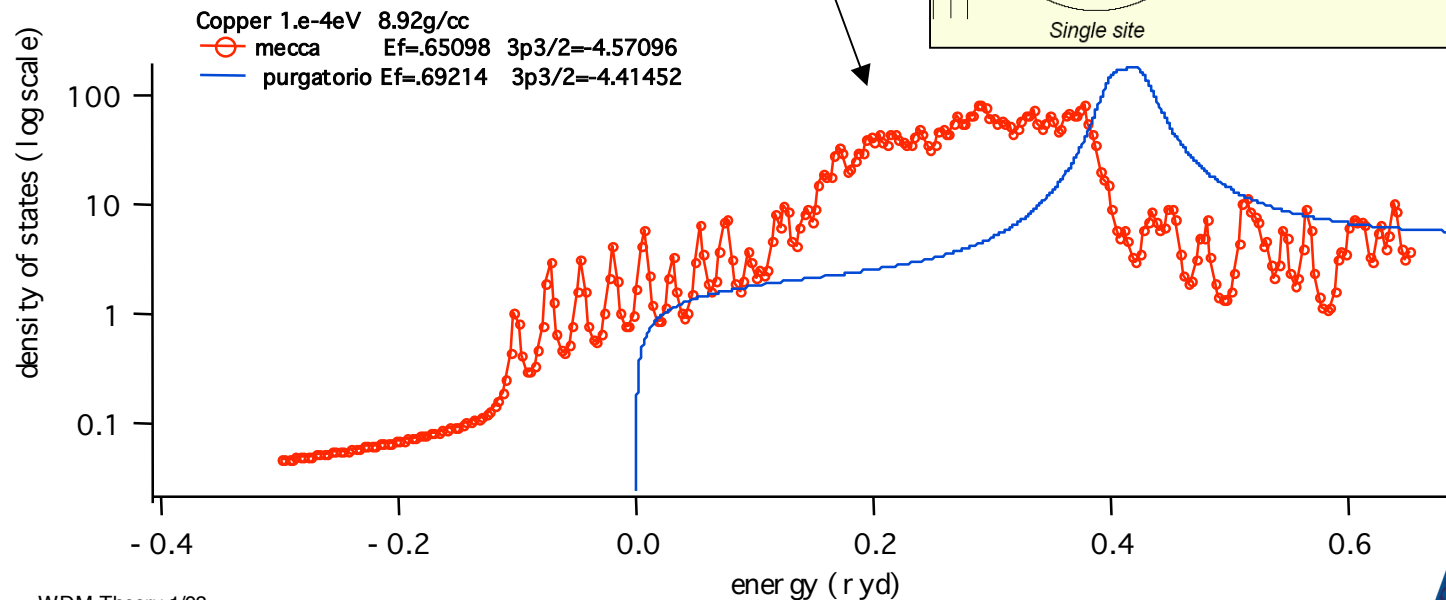
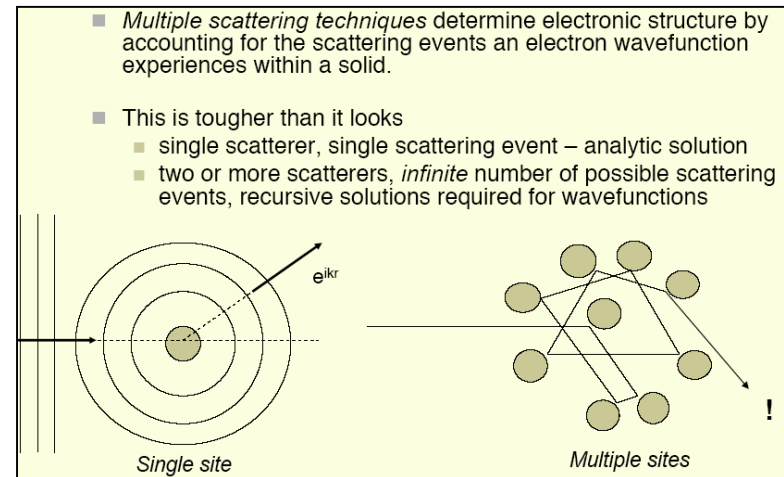


*Paradiso*

# Spatial Correlation Between Different Ion Centers Matter In Warm Dense Systems - How to Incorporate Multiple Centers?



- Multiple Ion Scattering has a Strong Effect in WDM systems.
- D. Johnson's KKR 'MECCA' code compared to PURGATORIO
- We are synthesizing his KKR code with the PURGATORIO algorithms/approach.\*



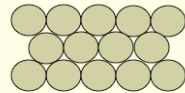
\*LLNL V  
Theory -  
Wilson et. al.  
& D. Johnson -  
UIUC

# Model Warm Dense Plasma as an Amorphous, Finite Temperature Metal using the Kohn-Korringa-Rostocker Multiple Scattering Green's Function Method with $O(N)$ methods and Improved Entropy.



## Atomic Sphere Approximations and Plasmas as amorphous metals

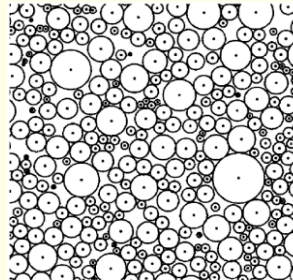
Many crystals are close-packed systems (fcc, bcc, and hcp)  
Most of the space is filled by atomic spheres



In a plasma we don't have periodicity and the luxury of Bloch's theorem.

One must generate positions and radii.

KKR approach works best when the system is close packed. Otherwise we have to pack the system with empty spheres to fill space



- In contrast to solid state we must compute electronic DOS over generated ensembles of spatially amorphous (non periodic) space-filling atomic spheres which represent the plasma

We need many and(or) large clusters(super-cells):

- with many accessible angular momentum channels
- All-Electron Treatment (no artificial separation Between core and valence)

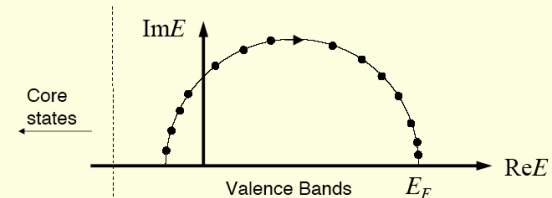
Matrix inversions along complex energy contour are independent  
⇒ massive parallel computation

## Integration in the Complex Plane

Charge density is determined by integrating the Green's function over energy.

However, on the real axis, Green's function is a very sharp function. If we move off the real axis, the Green's function becomes much smoother.

30 data points able to do the work of 1000's!



# The Kohn-Korringa-Rostocker Green's Function Method\*



## Move over Wavefunctions

$$G^R = [E - H]^{-1} \leftarrow \text{Off diagonal terms give you electron propagation,}$$

$$T = \text{Tr}[\Gamma_L G_{\text{LW}}^R \Gamma_R G_{\text{N1}}^A]$$

Diagonal elements give

$$\rho(r) = -\frac{1}{\pi} \int f(E - \varepsilon_F) \text{Im} G(\mathbf{r}, \mathbf{r}, E) dE \quad \text{Charge density}$$

$$n(E) = -\frac{1}{\pi} \int \text{Im} G(\mathbf{r}, \mathbf{r}, E) d^3\mathbf{r} \quad \text{Density of states}$$

From the charge, we can calculate the potential and perform self-consistent calculations

## Introducing the T matrix

We can rearrange the last equation to isolate the effects of the potential.

$$G = G_o + G_o(V + VG_oV + VG_oVG_oV + \dots)G_o \\ = G_o + G_oTG_o$$

where

$$T(V) = V + VG_oV + VG_oVG_oV + \dots$$

The scattering matrix, T, completely describes scattering within the potential assembly. It contains all possible scattering paths.

- \*[1] J. Korringa, *Physica* **13**, 392(1947) .[2] W. Kohn and N. Rostoker, *Phys. Rev.* **94**, 1111 (1954).  
[3] Johnson et al., PRL (1986); PRB (1990)  
[4] Johnson and Pinski, PRB (1993).  
[5] Ghosh et al. PRB (2005), Biava et al. PRB (2006)  
[6] Yang et al., PRL 75, 2867 (1995)  
[7] Moghadam et. al., J. Physics: Cond. Matter. **13**, 3073, (2001), other ORNL refs.

## All the possible paths...

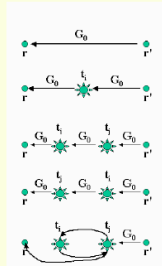
We can now write the T matrix in terms of the single site scattering matrix,  $t$ .

$$T\left(\sum_i V^i\right) = \sum_i t^i + \sum_i \sum_{j \neq i} t^i G_o t^j + \dots$$

This equation shows that the scattering matrix of an scattering assembly is made up of all possible scattering sequences.

Each scattering sequence involves scattering at individual cells with free electron propagation between.

$$T = \sum_{ij} T^{ij} \quad \text{where} \quad T^{ij} = t^i \delta_{ij} + t^i G_o \sum_{k \neq i} T^{kj}$$



## Getting the Band Together

In the MT formalism, the T matrix becomes:

$$T^{ij} = t^i \delta_{ij} + t^i \sum_{k \neq i} \tilde{G}^{ik} T^{kj}$$

There exists a matrix M such that  $T^{ij}$  are the elements of its inverse. The matrix m is just the inverse of the cell t matrix.

$$M^{ij} = m^i \delta_{ij} - \tilde{G}^{ij} (1 - \delta_{ij})$$

The inverse of the T matrix is cleanly separated into **potential** scattering components,  $m^i$ , and **structural** components,  $\tilde{G}^{ij}$ .

The poles of M determine the eigenenergies for the system for a given k through the following equation:

$$\det[m - \tilde{G}(k)] = 0$$

This allows us to calculate the system band structure.

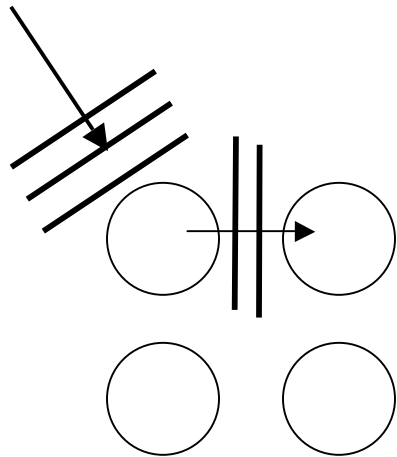
# Multiple-Scattering Theory (KKR Green's functions and $Y_{lm}$ scaling)



$$[-\nabla^2 + V(r) - E]G(r, r'; E) = \delta(r - r')$$

**Note:  $G(E)$  is complex and non-Hermitian**

**$E$  can be complex**



**Dyson t-matrices**

$$t(E) = t_{LL'}^i(E) \delta_{ij}$$

potential dependent

The positions,  $R_j$ , of the scatterers (now an amorphous MT 'foam') are given by free-space Green's function,  $G_0(R_{ij}; E)$ .

$$G_0^{ij}(E) = -\frac{1}{4\pi} \sum_{i \neq j} \frac{e^{i\kappa |R_i - R_j|}}{|R_i - R_j|} \quad \kappa = \sqrt{E}$$

• "free electron" wave scatters off site with a phase-shift,  $d_l(E)$ , and then is free again.

• wavefunction expanded on site as

$$\psi_{\mathbf{k}, \nu}(\mathbf{r}) = \sum_{L=(l, m)} c_{L, \nu}(\mathbf{k}) R_{l\nu}(r; E) Y_L(\hat{r})$$

• interstitial  $e^{i\mathbf{k} \cdot \mathbf{r}} = 4\pi \sum_L i^l j_l(kr) Y_L^*(\hat{k}) Y_L(\hat{r})$

For  $l \approx 3$  or  $4$ ,  $\delta_l(E) = 0$ , hence rather **compact basis**.

**Matrices have rank =  $N*(L+1)^2 \approx N*16$  or  $N*25$ .**



## The Main Challenge of Finite Temperature is an Efficient Way to Compute the Entropy from the KKR Foam Green's Functions via $f(E) \sim \text{Im } \int G$ . Pole Structure Reflects Physics!



- Determine  $F(T) = E(T) - TS(T)$
- Need Electronic Entropy:

$$S(T) = f(E) \ln f(E) - (1 - f(E)) \ln(1 - f(E)),$$

has a singularity at  $\omega_n = (2n+1)\pi k_B T$  with infinite branch-cut.  
So the farthest off for  $S(T)$  calculation is  $\pi k_B T/2$ .

- Also, can show that  $E(T=0) \sim E(T) - TS(T)/2$ .
- But does this speed up calculations and increase accuracy of the real-space  $O(N)$  method?

**No! Need entropy within first Matsubara pole (small  $\text{Im}$  , ill convergence).**



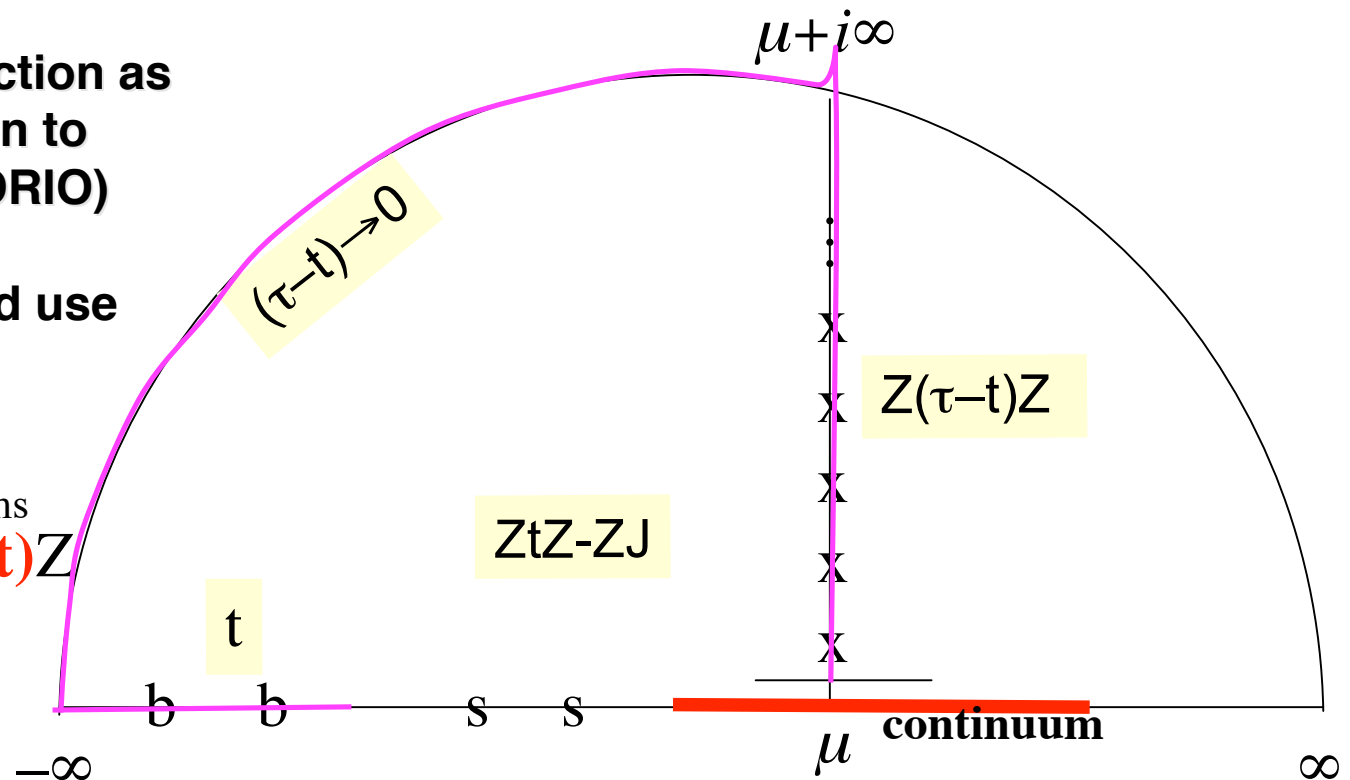
# Into the Complex Plane with Gun and Camera!



- Expand Green's Function as Multi-Center Correction to Single Site (PURGATORIO) Result.
- Multiple contours and use Jordan's Lemma

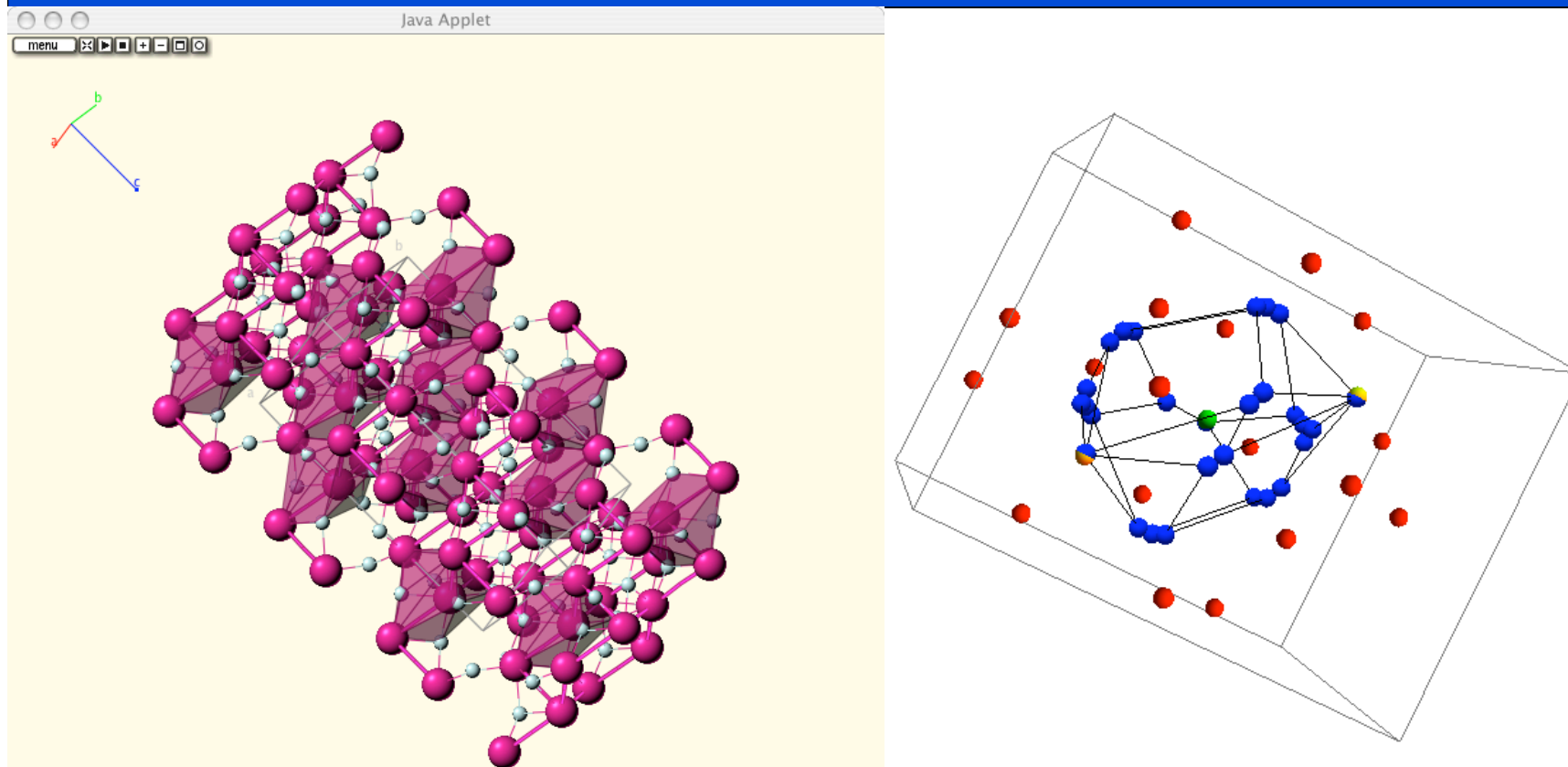
$$G = G_{ss} + G_{ms}$$

$$= (ZtZ - ZJ) + Z(\tau - t)Z$$



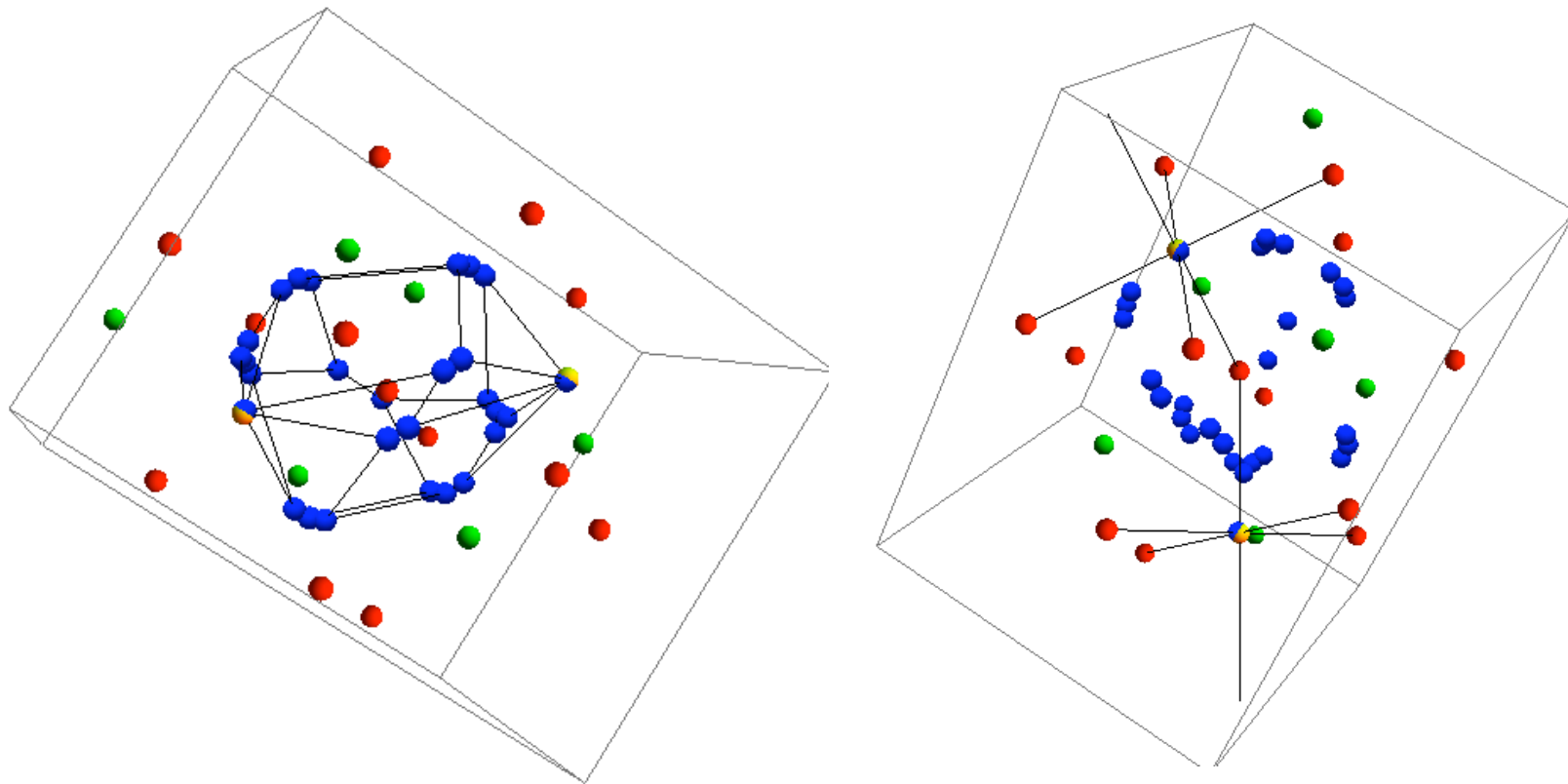
$$G = \sum_{\text{bound states}} G_{\text{core}} + \int dz (ZtZ - ZJ) + \sum Z(\omega_n) [\tau(\omega_n) - t(\omega_n)] Z(\omega_n)$$

# Voronoi Polyhedra for $\text{Al}_2\text{O}_3$ (corundum) Illustrate Typical 'Paradiso' Wigner-Seitz Cells $\rightarrow$ KKR MT (1)



- $\text{Al}_2\text{O}_3$  is a good test case - low Z, experiments, complex cell even for crystalline case.
- Corundum structure (left), Al (red), O (white)). Voronoi (WS cell) (right) surrounding central oxygen. Vertices **blue**, neighboring atoms **red**.

# Voronoi Polyhedra for $\text{Al}_2\text{O}_3$ (corundum) Illustrate Typical 'Paradiso' Wigner-Seitz Cells (2)



- Voronoi polyhedron surrounding central Oxygen (**red**) in corundum unit cell.
- Vertices are **blue**, Aluminum (**green**) and Oxygen (**red**) nearest neighbors are shown. Note tripling of vertices due to trigonal distortion and degenerate vertices equidistant to multiple atoms (right).

# “The Subject is Vast, but my Time is Brief...” (Erich von Stroheim in ‘Five Graves to Cairo’)



- In this brief talk, I’ve neglected two very important methods:
  - ACTEX (Activity Expansion) - F. Rogers
  - Thermal Field Theory (L. S. Brown et. al.)
- The ACTEX method goes after the Grand Partition Function, dealing with the Coulomb divergence of the Partition Function via the ‘Planck-Larkin’ method and via resummation accounts for composite particles on an equal footing.  $Z \sim \sum 2n^2 \exp(\text{Ryd}/n^2 kT) \rightarrow (\exp(-\beta E) - 1 + \beta E) + (1 - \beta E)$
- In Thermal Field Theory, one writes (and use dimensional regularization):

$$Z[\mu] = \int [d\phi] e^{-S[\phi; \mu]}. \quad (1)$$

Here the action  $S[\phi; \mu]$  is given by a functional integral over all the fields that correspond to all the elementary particles in the plasma,

$$e^{-S[\phi; \mu]} = \int [d\psi^* d\psi] e^{-W}, \quad (2)$$

with

$$W = \int_0^\beta d\tau \int (d^3\mathbf{r}) \left\{ \frac{1}{2} (\nabla \phi)^2 + \sum_a \psi_a^* \left[ \frac{\partial}{\partial \tau} - \frac{\nabla^2}{2m_a} - \mu_a - ie_a \phi \right] \psi_a \right\}. \quad (3)$$

The validity of this construction is easy to establish. The field  $\phi$  is coupled to the total charge density  $\rho = \sum_a e_a \psi_a^* \psi_a$ . Interchanging integrals and performing the Gaussian functional integral by completing the square yields

$$\begin{aligned} & \int [d\phi] \exp \left\{ - \int_0^\beta d\tau \int (d^3\mathbf{r}) \left[ \frac{1}{2} (\nabla \phi)^2 - i\phi \rho \right] \right\} \\ &= \exp \left\{ - \frac{1}{2} \int_0^\beta d\tau \int (d^3\mathbf{r}) \int (d^3\mathbf{r}') \rho(\mathbf{r}, \tau) V_C(\mathbf{r} - \mathbf{r}') \rho(\mathbf{r}', \tau) \right\}, \end{aligned} \quad (4)$$

where  $V_C(\mathbf{r} - \mathbf{r}')$  is the Coulomb potential. The resulting functional integral over the matter fields  $\psi^*, \psi$  is the standard functional integral representation for the partition function.

WUM theory 1/08

$$Z[\mu] = \int [d\phi] e^{-S_{\text{eff}}[\phi; \mu]}. \quad (5)$$

Since the thermal wave lengths are proportional to Planck’s constant  $\hbar$ , the leading term in this expansion is the classical limit,  $S_{\text{eff}}[\phi; \mu] \rightarrow S_{\text{cl}}[\phi; \mu]$ , which is found [1] to be

$$S_{\text{cl}}[\phi; \mu] = \int_0^\beta d\tau \int (d^3\mathbf{r}) \left[ \frac{1}{2} (\nabla \phi(\mathbf{r}, \tau))^2 - \frac{1}{\beta} \sum_a n_a^0 e^{i\beta e_a \phi(\mathbf{r})} \right], \quad (6)$$

in which the sum runs over all the particles species  $a$  in the plasma,  $n_a^0 = (g_a/\lambda_a^3) e^{\beta \mu_a}$  are the particle densities in the free-particle limit with  $g_a$  the spin degeneracy, and  $\lambda_a = \hbar(2\pi\beta m_a)^{1/2}$  is the thermal wave length, while

$$\phi(\mathbf{r}) = \frac{1}{\beta} \int_0^\beta d\tau \phi(\mathbf{r}, \tau) \quad (7)$$

# Some High Energy Density and Warm Dense Matter Physics References



“Physics of Shock Waves & High Temperature Hydrodynamic Phenomena” by Ya. B. Zeldovich & Yu. P. Raizer, (edited by W. D. Hayes & R. F. Probstein) Academic Press, NY (1966).

- R. Jeanloz, Physics Today 53, 44 (2000)
- M. D. Rosen, Phys. Plasmas 6, 1690 (1999), Phys. Plasmas 3, 1803 (1996)
- E. M. Campbell, N. C. Holmes, S. B. Libby, B. A. Remington, E. Teller, "The Evolution of High Energy Density Physics: from Nuclear Testing to the Superlasers," Lasers and Particle Beams, (1997), 15, No. 4, 607.
- D. A. Liberman, PRB 20, 4981, (1979)
- B. Wilson, V. Sonnad, P. Sterne, and W. Isaacs, JQSRT 99, 658-679, (2006).
- See the many KKR, O(N) methods, and other PARADISO relevant references above (KKR, Stocks et. al., Andersen, Yang, Zeller, Johnson, ...,et. al)
- L. S. Brown, L. Yaffe, Phys. Rep. 340, 1-164, (2000) and subsequent refs.
- F. Rogers, Phys. Rev., Phys. Plasmas, 7, 51, (2000) and refs therein.
- and of course, R. M. More, (many references from his lectures), M. Desjarlais, M. Murillo (references in their lectures),...

# Challenges and Virtues of KKR Green's Function Method



## Problems with the KKR approach

- Linking interstitial region ( $V=0$ ) with spherical regions with muffin tin potentials can be difficult
- Determinant used to find band structure is a non-linear function of energy (energy dependence carried in the site  $t$  matrices) – *this can not be reduced to a standard matrix eigenvalue problem*
- *The Solution* – Linearize the equation – LMTO approach (Andersen, PRB, 1975 – 1370 citations)

- **Extensions beyond the independent electron approximation (e.g. DynamicalMeanFieldTheory) can be pursued**

- **No ad hoc continuum lowering models**
- **Non muffin tin (“Full Potential”) extensions can be pursued**

## Benefits of Green's Function Approach

- Capable of Handling Open Systems (something periodic DFT codes have trouble with)
- System Properties (electronic charge, density of states, etc) without using wavefunctions
- Ability to Handle Different Scattering Mechanisms through Self Energy Terms (not discussed here)
- Natural Formalism for Transport Calculations